Ceramide Synthase 6 Knockdown Suppresses Apoptosis after Photodynamic Therapy in Human Head and Neck Squamous Carcinoma Cells

DUSKA SEPAROVIC[1,2], PAUL BREEN[1*], NICHOLAS JOSEPH[1*], JACEK BIELAWSKI[3], JASON S. PIERCE[3], ERIC VAN BUREN[2] and TATYANA I. GUDZ[4,5]

[1]*Department of Pharmaceutical Sciences, Eugene Applebaum College of Pharmacy and Health Sciences, and* [2]*Karmanos Cancer Institute, Wayne State University, Detroit, MI, U.S.A.;* [3]*Department of Biochemistry and Molecular Biology,* [4]*Ralph H. Johnson Veterans Affairs Medical Center, and* [5]*Department of Neuroscience, Medical University of South Carolina, Charleston, SC, U.S.A.*

Abstract. *Background: The effectiveness of photodynamic therapy (PDT) for cancer treatment correlates with apoptosis. We observed that suppression of de novo-generated sphingolipids, e.g. ceramide, renders cells resistant to apoptosis post-PDT. Ceramide synthase 6 (CerS6) has been implicated in apoptosis after various stimuli. Aim: To investigate the involvement of down-regulation of CerS6 in apoptosis and its impact on the sphingolipid profile post-PDT with the silicone phthalocyanine Pc 4 in a human head and neck squamous carcinoma cell line. Materials and Methods: Besides siRNA transfections and PDT treatment, immunoblotting for protein expression, mass spectrometry for sphingolipid analysis, spectroflurometry and flow cytometry for apoptotic marker detection, and trypan blue assay for cytotoxicity assessment, were used. Results: CerS6 knockdown led to reduction in PDT-induced DEVDase activation, mitochondrial depolarization, apoptosis and cell death. CerS6 knockdown was associated with selective decreases in ceramides and dihydroceramides, markedly of C18-dihydroceramide, post-PDT. Conclusion: CerS6 might be a novel therapeutic target for regulating apoptotic resistance to PDT.*

*These authors contributed equally to this paper.

Correspondence to: Duska Separovic, Department of Pharmaceutical Sciences, Eugene Applebaum College of Pharmacy and Health Sciences, Wayne State University, 259 Mack Ave., Detroit, MI 48201, U.S.A. Tel: +1 3135778065, Fax: +1 3135772033, e-mail: dseparovic@wayne.edu

Key Words: Apoptosis, ceramide, ceramide synthase 6, dihydroceramide, PDT, sphingolipids, head and neck squamous carcinoma, UM-SCC-22A cells.

Sphingolipids, *e.g.* ceramide, modulate biological processes, including apoptotic cell death (1, 2). A major route of ceramide generation is the *de novo* sphingolipid biosynthesis pathway (Figure 1), in which ceramide synthase (CerS) acylates dihydrosphingosine to give rise to dihydroceramide, which is then oxidized to yield ceramide. There are six CerS isoforms showing fatty acyl CoA preferences (3), which have been implicated in distinct biological functions (4, 5). Specifically, CerS6 has been implicated in apoptosis after various stimuli, including tumor necrosis factor-related apoptosis-inducing ligand (TRAIL), glutamate and nerve growth factor (6, 7).

The *de novo* sphingolipid biosynthesis pathway affects the response to anticancer drugs (8, 9), including photodynamic therapy (PDT) (10-12). PDT utilizes a photosensitizer, visible light and oxygen to generate reactive oxygen species that can destroy malignant cells by apoptosis (13, 14). The effectiveness of PDT regimens correlates with tumor cell apoptosis (15). Using pharmacological and genetic approaches, we have demonstrated that *de novo* sphingolipid modulate apoptosis after PDT with the silicone phthalocyanine Pc 4 photosensitizer (10-12). However, the role of CerS6 in PDT-induced apoptosis is not known. In the present study, we tested the role of *CerS6* knockdown in regulation of apoptotic cell death and the sphingolipid profile after Pc 4-PDT in UM-SCC-22A, a human head and neck squamous carcinoma cell line.

Materials and Methods

Materials. Pc 4, $HOSiPcOSi(CH_3)_2(CH_2)_3N(CH_3)_2$, was kindly supplied by Dr. Malcolm E. Kenney (Case Western Reserve University, Cleveland, OH, USA). Dulbecco's modified Eagle's medium (DMEM) and serum were from Invitrogen Life Sciences (Grand Island, NY, USA) and Hyclone (Logan, UT, USA), respectively. UM-SCC-22A, a human head and neck squamous carcinoma cell line from hypopharynx (16, 17), was kindly supplied by Dr. Thomas Carey (University of Michigan, Ann Arbor, MI, USA).

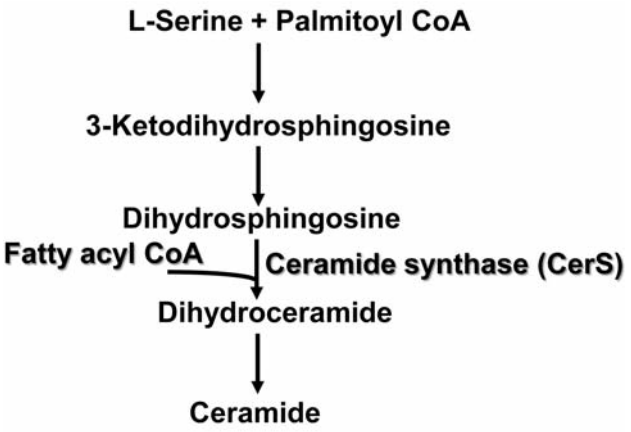

Figure 1. *The de novo sphingolipid biosynthesis pathway.*

Cell culture. UM-SCC-22A cells were grown in DMEM medium containing 10% fetal bovine serum, 1% non-essential amino acids, 100 units/ml penicillin, and 100 μg/ml streptomycin. Cells were maintained at 37˚C in an incubator with a 5% CO_2 atmosphere, and were treated in the growth medium.

siRNA transfection and PDT treatment. The siRNA targeting the sequence AAG GCA CCA AAA AGT ACC CGG of human *CerS6* was from Qiagen (Valencia, CA, USA). In addition, to verify *CerS6* knockdown effects, siGenome SMART pool silencing RNA was purchased from Thermo Scientific/Dharmacon (Lafayette, CO, USA). The pool contains three siRNAs targeting different sequences of human CerS6. For control siRNA, AllStars Negative Control siRNA from Qiagen was used. UM-SCC-22A cells were transfected with double-strand siRNAs using Oligofectamine from Invitrogen Life Sciences according to the manufacturer's instructions. The protocol was optimized regarding the concentration of siCerS6, transfection and post-transfection conditions in preliminary dose-response experiments (10-100 nM siCerS6). Consequently, the following protocol was employed: cells (1×10^6) were transfected with 25 nM of each siRNA. Twenty-four hours after transfection, cells were collected and seeded in fresh growth medium. Following overnight exposure to Pc 4 (250 and 500 nM), cells were irradiated with red light (2 mW/cm^2; λ_{max} ~670 nm) using a light-emitting diode array (EFOS; Mississauga, ONT, Canada) at a fluence of 200 mJ/cm^2 at room temperature. Following PDT, cells were incubated at 37˚C for 2 or 24 hours, rested on ice and processed for various analyses. For mass spectrometric analysis, cells were washed twice with cold phosphate-buffered saline, resuspended in a mixture of ethyl acetate/methanol (1:1, v/v), dried under nitrogen, and shipped overnight on dry ice to the Lipidomics Shared Resource (Medical University of South Carolina, Charleston, SC, USA) for further processing.

Sphingolipid analysis by quantitative high performance liquid chromatography (HPLC)/mass spectrometry (MS). Following extraction, sphingolipids were separated by HPLC, introduced to electrospray ionization source and then analyzed by double MS using TSQ 7000 triple quadrupole mass spectrometer from Thermo-Fisher Scientific (Waltham, MA, USA) as described previously (18).

Immunoblotting. Following PDT, cells were collected, lysed in reducing Laemmli buffer, boiled and then subjected to sodium dodecyl sulfate polyacrylamide gel electrophoresis (SDS-PAGE) and western immunoblotting, as reported previously (11, 19). Equal protein loading was confirmed using anti-pan-actin. The following antibodies were obtained from Novus Biologicals (Littleton, CO, USA): anti-CerS1 and anti-CerS6 (mouse polyclonal each); antiCerS2 (mouse monoclonal); anti-CerS5 (rabbit polyclonal). These antibodies were originally made by Abnova (Taipei City, Taiwan, ROC). Mouse monoclonal anti-pan-actin was from Neo Markers (Kalamazoo, MI, USA). Following visualization of blots using ECL Plus chemifluorescence kit and STORM 860 imaging system (GE Healthcare, Piscataway, NJ, USA) they were quantified by ImageQuant 5.2 (GE Healthcare).

DEVDase (caspase-3-like) activity assay. After PDT, cells were harvested and lysed in radio immunoprecipitation assay (RIPA) buffer. Following centrifugation (10,000 ×g), cytosolic fraction was obtained, and DEVDase activity was determined by an assay based on the enzyme's cleavage of a fluorogenic derivative of the tetrapeptide substrate Asp-Glu-Val-Asp [Ac-DEVD-AMC (7-amino-4-methylcoumarin)] from Enzo Life Sciences (Farmingdale, NY, USA) (11). The fluorescence of the cleaved DEVD substrate was measured using an F-2500 spectrofluorometer (Hitachi; Dallas, TX, USA) (380 nm excitation, 460 nm emission).

Mitochondrial membrane depolarization measurement. The lipophilic cationic dye JC-1 (5,5',6,6'-tetrachloro-1,1'3,3'-tetraethylbenzimidazo-lylcarbocyanine iodide) was used to determine mitochondrial membrane potential by flow cytometry, as we described previously (12). In normal mitochondria with a high negative membrane potential, JC-1 produces aggregates that emit a red fluorescence (590 nm). In mitochondria with low membrane potential (depolarized mitochondria), the dye generates monomers in the cytosol that emit a green fluorescence (527 nm) (20). Following PDT, cells were harvested and processed for flow cytometry according to the manufacturer's instructions (BD Biosciences, San Diego, CA, USA). BD LSR II flow cytometer was used for the analysis (BD Biosciences).

Apoptosis detection. As we showed previously (21, 22), to detect apoptosis, the exposure of phosphatidylserine in the outer leaflet of the cell membrane was measured using annexin V, a protein which binds with high affinity to negatively charged phosphatidylserine in the presence of calcium. As apoptosis progresses, cell membrane integrity is lost, and this can be detected using DNA-binding fluorescent dye propidium iodide (PI, red fluorescence). By attaching annexin V to fluorescein isothiocyanate (green fluorescence), one can discriminate between intact cells (annexin V^-/PI^-), early apoptotic (annexin V^+/PI^-), and late apoptotic or necrotic cells (annexin V^+/PI^+). The kit was purchased from BD Pharmingen (BD Biosciences) and the flow cytometric protocol was followed, as described by the manufacturer.

Trypan blue dye exclusion assay. After PDT, cells were harvested, resuspended in cell growth medium, and diluted 1:1 with 0.4% trypan blue stain from Sigma-Aldrich (St. Louis, MO, USA). Stained and unstained cells were counted using a hemocytometer. Trypan blue-positive cells were considered to be dead cells.

Statistical analysis. Following data collection, the average value of untreated and each treated group and the standard error were calculated for at least n=3. Data were analyzed for statistically

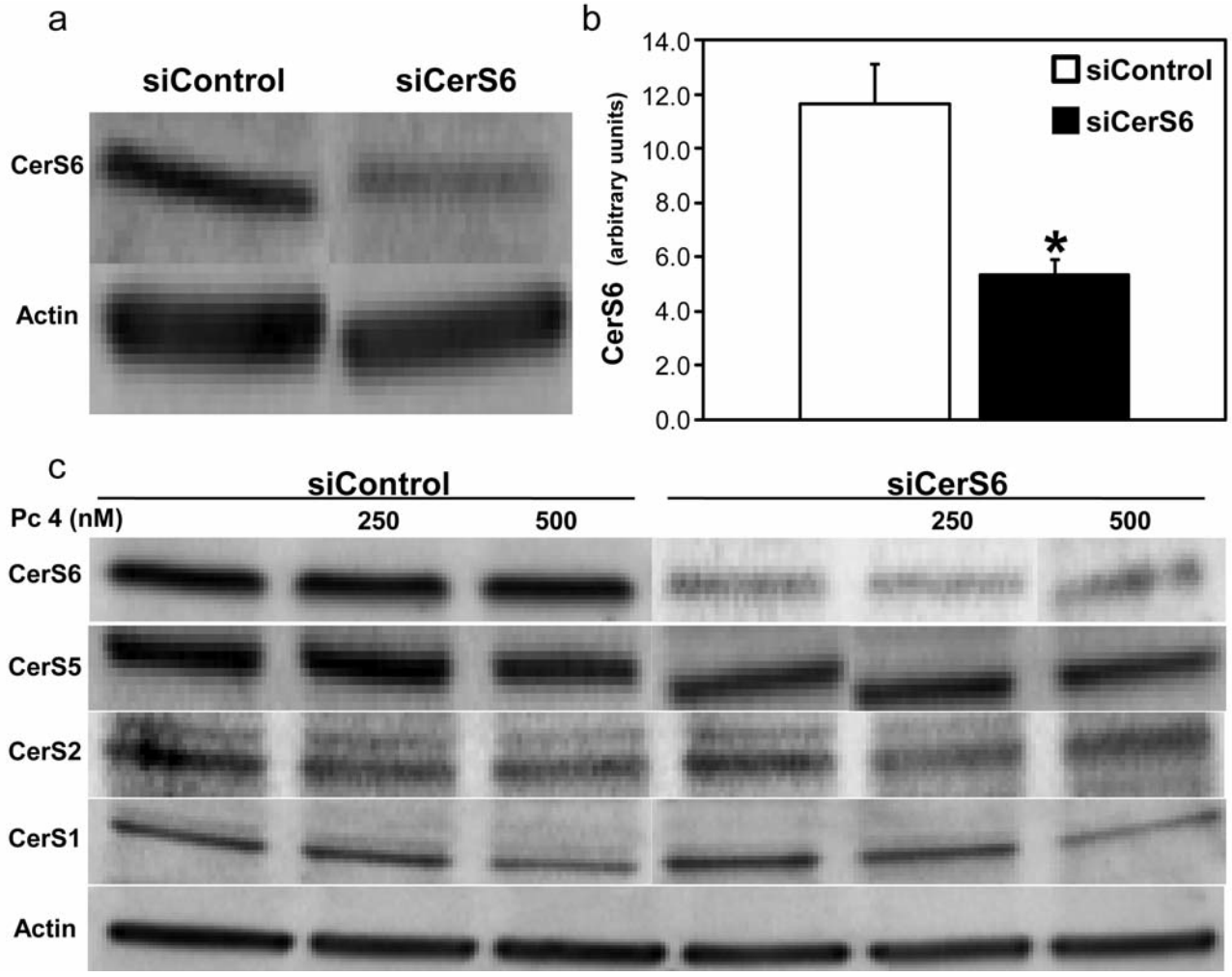

Figure 2. *Effect of ceramide synthase 6 (CerS6) knockdown and photodynamic therapy (PDT) on expression of ceramide synthases. UM-SCC-22A cells were transfected with siRNA targeted against non-targeted control (siControl; 25 nM) or CerS6 (siCerS6; 25 nM). Twenty-four hours after transfection, cells were collected and seeded in fresh growth medium. a and b: Cells were incubated at 37˚C for an additional 24 hours prior to collection. c: After overnight exposure to Pc 4 (250 and 500 nM), cells were irradiated with red light (2 mW/cm^2). Following PDT, cells were incubated at 37˚C for two hours, collected on ice and processed for PAGE/western immunoblotting. Equal protein loading was verified using anti-pan-actin. a: Knockdown of CerS6 was confirmed in seven independent experiments. b: CerS6 protein levels were quantified from the blots and expressed in arbitrary units. The data are shown as the mean±SEM, *p≤0.05, n=11. c: Western blots of CerS1, CerS2, CerS5 and CerS6 in siControl- and siCerS6-tranfected cells are shown. Representative blots from 2-14 independent determinations are shown.*

significant differences between groups using Student's *t*-test of unequal variance. Statistical significance was ascribed to the data when $p \leq 0.05$.

Results

Effect of CerS6 knockdown and PDT on ceramide synthase expression. To verify down-regulation of CerS6 by RNA interference in UM-SCC-22A cells, expression levels of the protein were determined using immunoblotting. As shown in Figure 2a and b, CerS6 levels were reduced by 52% after *CerS6* knockdown. PDT had no effect on CerS6 expression in either siControl- or siCerS6-transfected cells (Figure 2c).

To test for potential off-target effects, expression levels of CerS1, -2, and -5 were determined using immunoblotting. As shown in Figure 2c, expression of CerS1 and CerS2 was not affected by *CerS6* knockdown. CerS5 levels were only marginally down-regulated after *CerS6* knockdown. Following PDT (500 nM Pc 4 + 200 mJ/cm^2), only CerS1 levels were slightly reduced in both siControl- and siCerS6-transfected cells.

CerS6 knockdown suppressed DEVDase activation after PDT. Although CerS6 has been implicated in apoptosis (5, 7), the involvement of CerS6 in PDT-induced apoptosis is unknown. We first examined the effect of *CerS6* knockdown

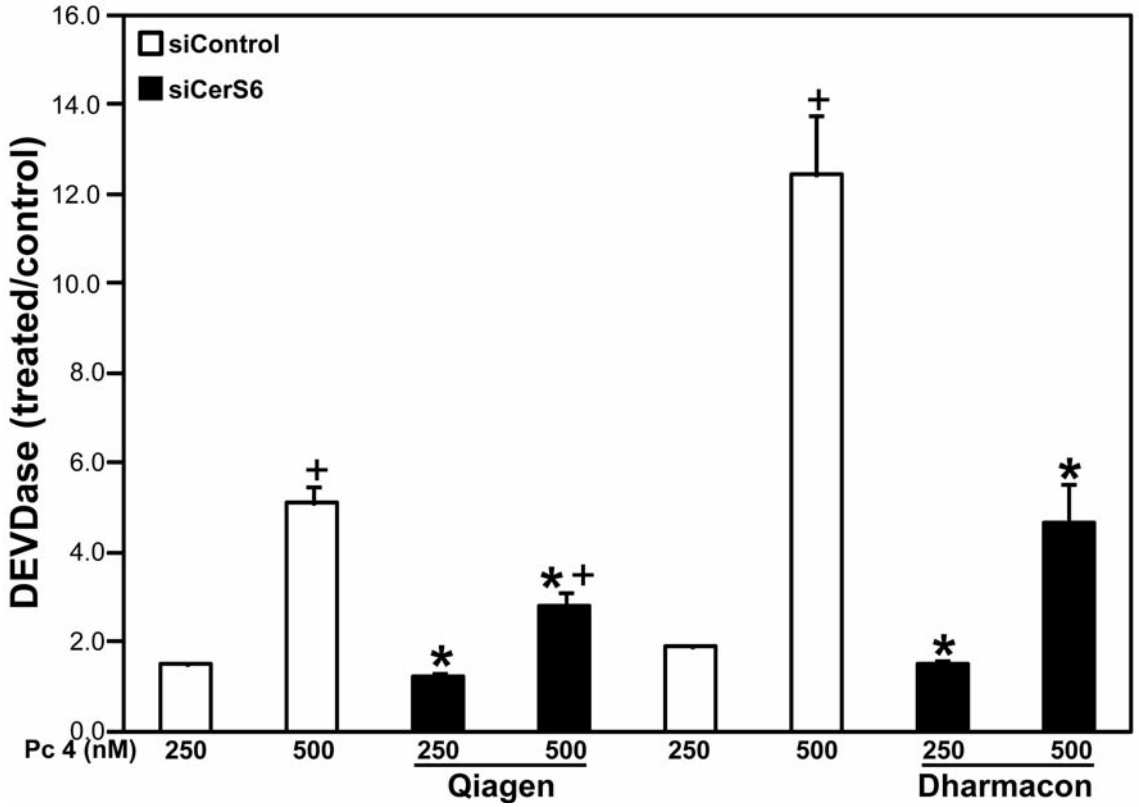

Figure 3. *Ceramide synthase 6 (CerS6) knockdown suppressed DEVDase activation after photodynamic therapy (PDT). Following 2-h incubations post-PDT, cells were collected, cell lysates were prepared and DEVDase activity was measured using Ac-DEVD-AMC as the fluorogenic substrate. Qiagen and Dharmacon refer to the corresponding siCerS6s used for transfections. The data are expressed as ratios of PDT-treated versus untreated controls and are presented as the mean±SEM, n=3-8. The significance (p≤0.05) is indicated as follows: *PDT-induced DEVDase activation is reduced by CerS6 knockdown; +DEVDase activation is different at two PDT doses.*

on DEVDase (caspase-3-like) activity after PDT. We found that at 2 h after PDT, DEVDase activation was significantly inhibited by CerS6 knockdown (Figure 3). The effect was reproduced in cells transfected with siGenome SMART pool of siCerS6 (Dharmacon). These findings support the involvement of CerS6 in activation of DEVDase post-PDT.

CerS6 knockdown suppressed mitochondrial depolarization, apoptosis and cell death after PDT. The loss of mitochondrial membrane potential is associated with PDT-evoked apoptosis (12, 23). We asked whether CerS6 affects apoptosis at the mitochondrial level after PDT. We found that PDT-induced mitochondrial depolarization was suppressed by *CerS6* knockdown not at 2 h (not shown) but at 24 h (Figure 4a). The data suggest that *CerS6* knockdown-dependent suppression of mitochondrial depolarization was preceded by its inhibition of DEVDase activation after PDT.

We further investigated the role of CerS6 in apoptosis after PDT using the apoptotic marker annexin V. Flow cytometric data revealed that *CerS6* knockdown led to significant reductions in the appearance of annexin V^+/PI^- and annexin V^+/PI^+ cells at 24 h after PDT (Figure 4b). These findings support the notion that *CerS6* knockdown yields the cells resistant to early and late apoptosis post-PDT.

To assess the effect of *CerS6* knockdown on short-term cell viability post-PDT, trypan blue dye exclusion assay was used. We found that following PDT the appearance of trypan blue-positive cells was attenuated by *CerS6* knockdown at 24 h (Figure 4c). Thus, *CerS6* knockdown was able to suppress cytotoxicity after PDT.

Effect of CerS6 knockdown on resting C16-ceramide levels and PDT-induced accumulation of global ceramides and dihydroceramides. To determine the effect of *CerS6* knockdown on the sphingolipid profile, resting levels of ceramide and dihydroceramides were measured by MS. Of all ceramides tested, *CerS6* knockdown significantly reduced only C16-ceramide levels (Figure 5a). The data are consistent with CerS6 being responsible for C16-ceramide generation.

We then explored the effect of PDT on the sphingolipid profile in cells transfected with siControl- or siCerS6. The data presented here were obtained at 2 h post-PDT. *CerS6*

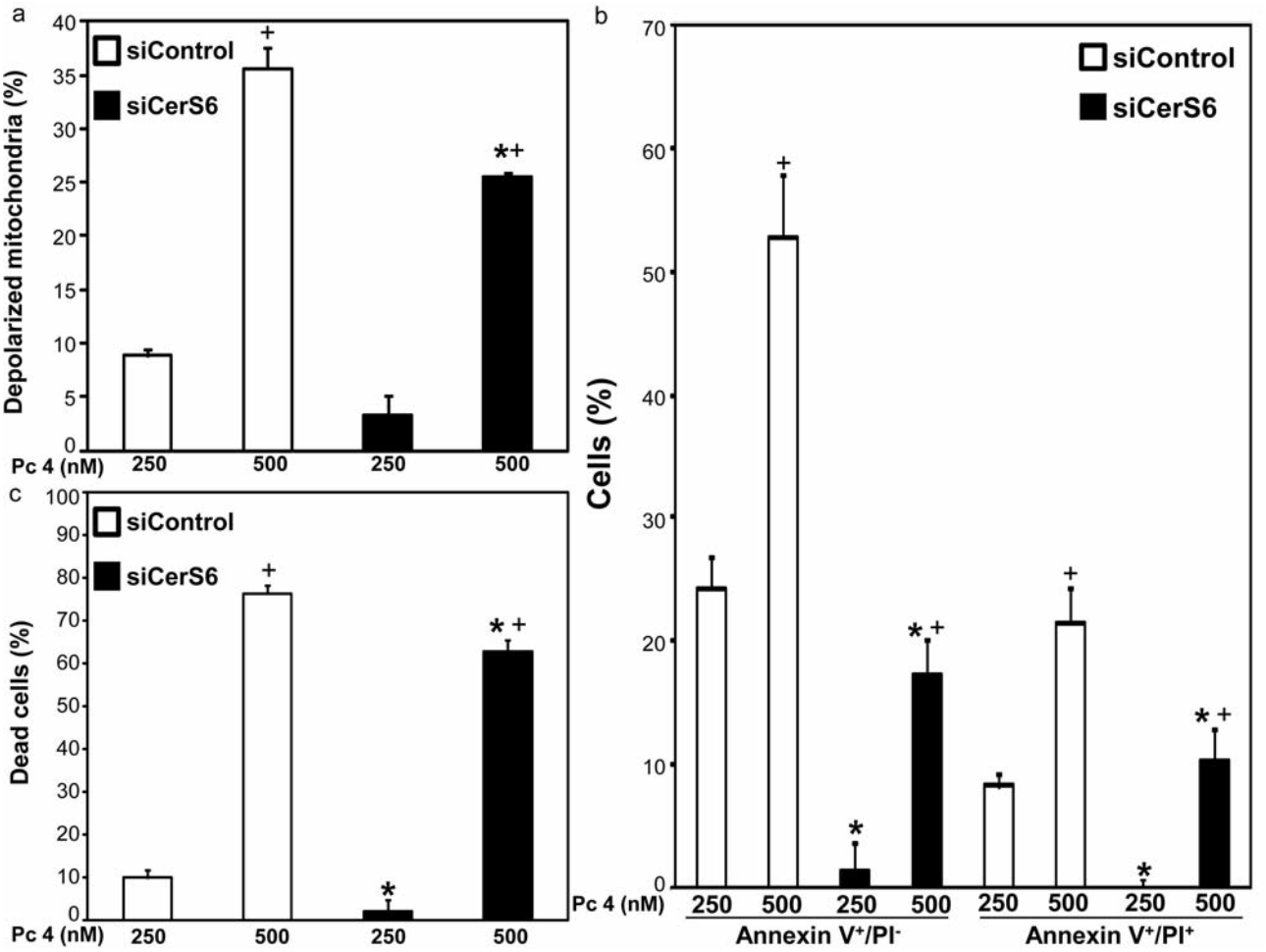

Figure 4. *Ceramide synthase 6 (CerS6) knockdown suppressed mitochondrial depolarization, apoptosis and cell death after photodynamic therapy (PDT). Following 24-h incubations post-PDT, cells were collected and processed for flow cytometry (a, b) or stained with trypan blue and counted (c). JC-1 and annexin V/propidium iodide (PI) staining were used to detect mitochondrial membrane potential (a) and apoptosis (b), respectively. In all panels data are shown as the mean±SEM, n=3-6. The significance (p≤0.05) is indicated as follows: *CerS6 knockdown suppresses PDT-induced mitochondrial depolarization, apoptosis or cell death; +mitochondrial depolarization, apoptosis or cell death is different at two PDT doses.*

knockdown attenuated global accumulation of ceramides and dihydroceramides after PDT (Figure 5b). Among all ceramides and dihydroceramides tested, PDT induced the greatest increase in C18-dihydroceramide (Figure 6). The 56-fold increase in C18-dihydroceramide after PDT was substantially reduced by *CerS6* knockdown. *CerS6* knockdown also significantly reduced PDT-induced accumulation of the following dihydrocetamides: C20-, C22-, C22:1-, C24-, C24:1- and C26:1-dihydroceramide. Furthermore, CerS6 knockdown elevated levels of the CerS substrate dihydrosphingosine after PDT (not shown).

PDT-induced accumulation of the following ceramides was significantly suppressed by *CerS6* knockdown: C18-, C20-, C20:1- and C26:1-ceramide (Figure 6). The effects of *CerS6* knockdown on accumulation of other ceramides and dihydroceramides did not correlate with reduced functional responses (not shown). Taken together, *CerS6* knockdown was associated with selective decreases in individual ceramides and dihydroceramides, in particular of C18-dihydroceramide, as well as with global decreases in ceramides and dihydroceramides after PDT.

Discussion

The key finding of our present study is that *CerS6* knockdown suppresses apoptotic cell death post-PDT. Although CerS1 was down-regulated after treatment of cells with the higher PDT dose, this occurred in siControl- and siCerS6-transfected cells, and therefore, does not account for observed differences in their apoptotic responses. Our present data indicate the

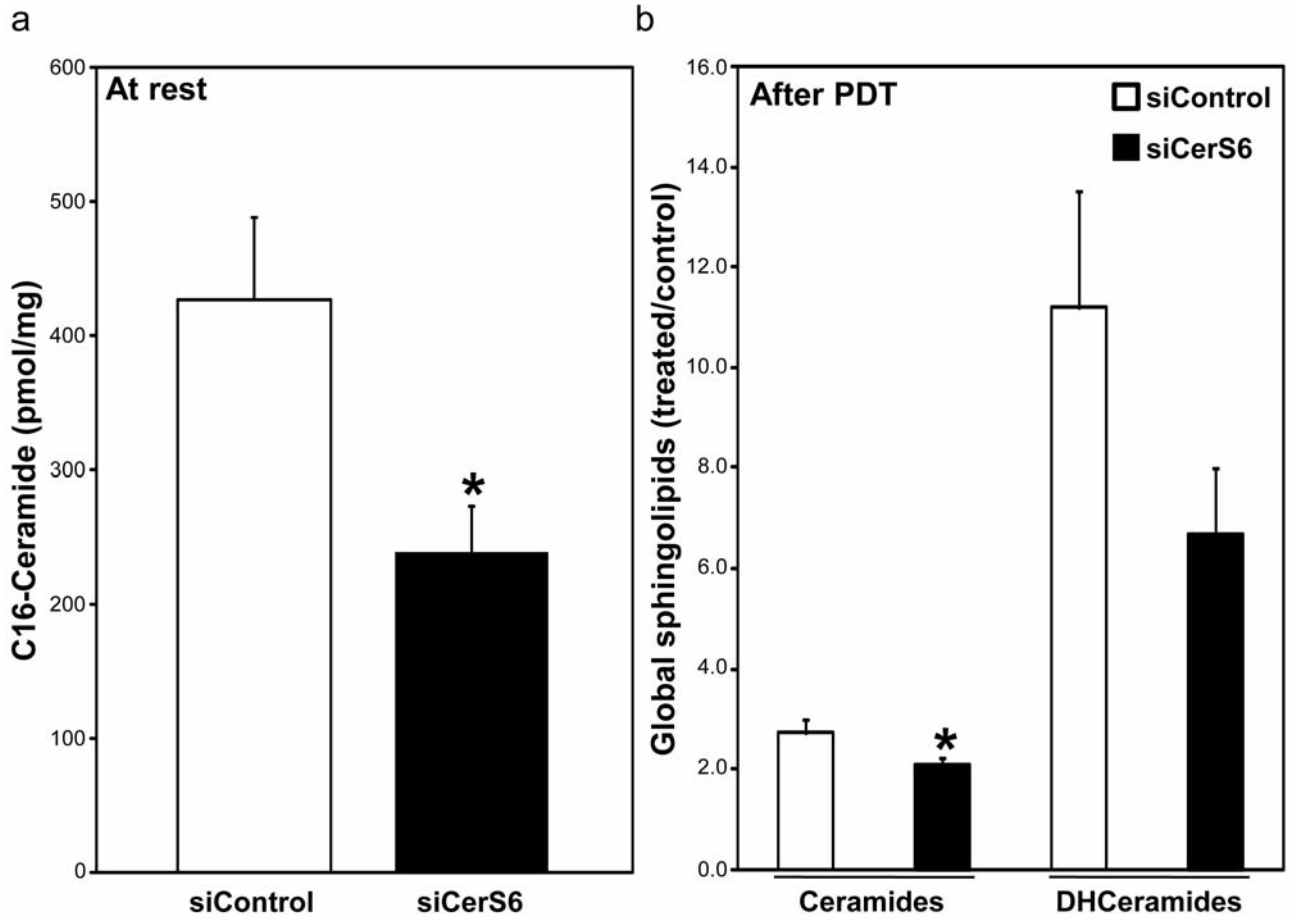

Figure 5. *Effect of ceramide synthase 6 (CerS6) knockdown on resting C16-ceramide levels (a) and photodynamic therapy (PDT)-induced accumulation of global ceramides and dihydroceramides (DHceramides) (b). a: Resting C16-ceramide levels obtained from untreated and Pc 4-treated (dark control) cells are expressed as pmol/mg. b: Following 2 h-incubations post-PDT (500 nM Pc 4 + 200 mJ/cm^2), cells were collected and processed for MS. The data are expressed as ratios of PDT-treated versus untreated controls. In both panels, the data are shown as the mean±SEM, n=3-4. *Indicates that CerS6 knockdown suppresses resting C16-ceramide levels or PDT-induced global ceramide accumulation at p≤0.05.*

involvement of CerS6 in apoptotic susceptibility. This is in line with our previous work showing the involvement of CerS6 in promoting apoptosis after treatment with glutamate and nerve growth factor (7). Similarly, *CerS6* knockdown inhibits TRAIL-induced apoptosis (6).

In contrast to the present findings, CerS6 has been shown to have an antiapoptotic role in endoplasmic reticulum (ER) stress responses (24, 25). Unlike PDT-induced apoptosis (26), ER stress response-evoked apoptosis includes transcriptional/ translational signaling, which could account for the apparently opposite role of CerS6 in apoptosis. Low levels of CerS6 have been proposed to affect translocation of activated caspase-3 into the nucleus (6). Our finding that *CerS6* knockdown inhibits DEVDase (caspase3-like) activation paves the way for future studies addressing the putative role of CerS6 in regulating nuclear permeability for caspase-3.

Mammalian CerS6 has been shown to utilize C16-, C14- and C18-CoA preferentially (27). Reduced basal levels of C16-ceramide by *CerS6* knockdown support specificity of the enzyme for C16-CoA in resting cells. However, specificity of CerS6 for C16-ceramide was not observed following PDT. *CerS6* knockdown was associated with decreases in ceramides (and dihydroceramides) other than C16-ceramide. On the other hand, decreases in PDT-induced C18-ceramide levels by *CerS6* knockdown support the idea of preferential utilization of C18-CoA by CerS6. Major changes in C18-ceramide that we discovered after PDT are in agreement with previous findings showing correlation between increases in C18-ceramide and inhibition of growth by mitochondrial apoptosis in UM-SCC-22A cells (28). Moreover, *CerS6* knockdown induced decreases in global ceramides and dihydroceramides after PDT. In contrast, *CerS6* knockdown increased total ceramides after UV

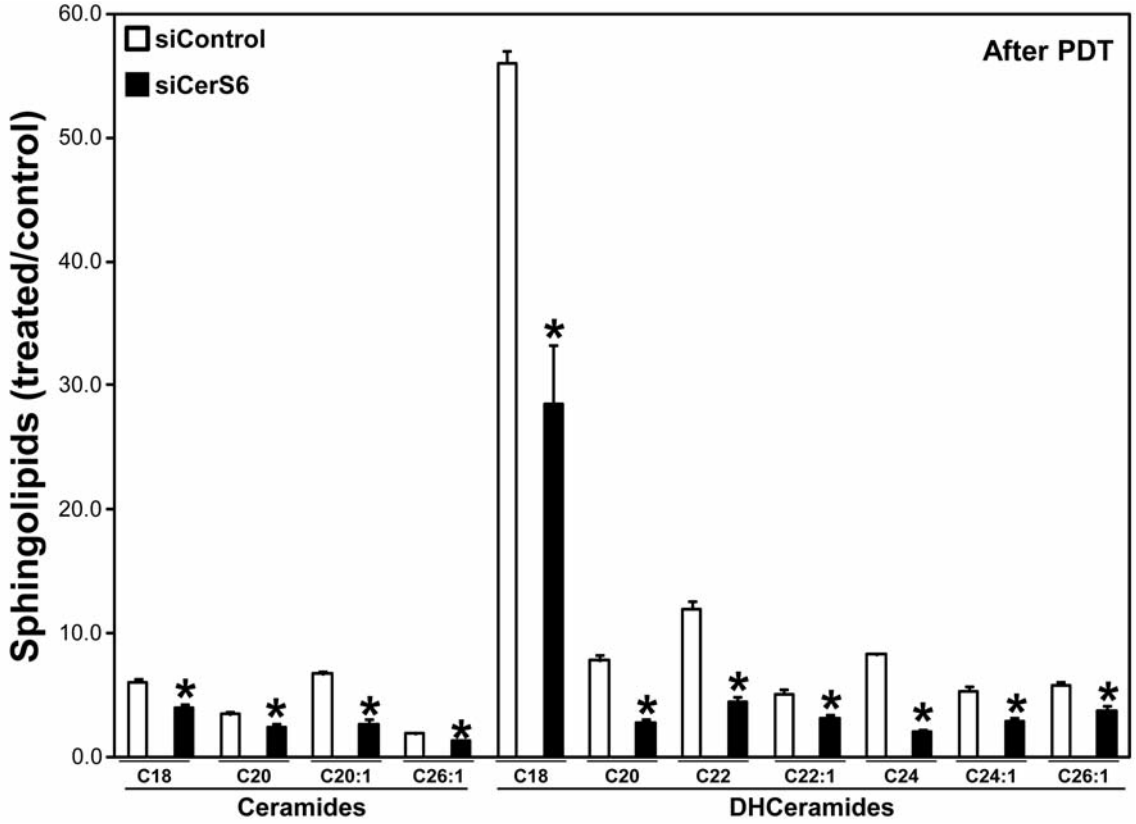

Figure 6. *Ceramide synthase 6 (CerS6) knockdown inhibits photodynamic therapy (PDT)-induced accumulation of ceramides and dihydroceramides (DHceramides). Following 2-h incubations post-PDT (500 nM Pc 4 + 200 mJ/cm^2), cells were collected and processed for MS. The data are expressed as ratios of PDT-treated versus untreated controls and are shown as the mean±SEM, n=3-4. *Indicates that CerS6 knockdown suppresses PDT-induced accumulation of corresponding ceramide or dihydroceramide at p≤0.05.*

irradiation (29). In the absence of differences in expressions of other CerSs between cells transfected with control- or CerS6-siRNA, observed wide range of changes in ceramides and dihydroceramides by *CerS6* knockdown suggest relaxation of substrate specificity of the enzyme after PDT, as proposed elsewhere (4).

The involvement of the *de novo* sphingolipid biosynthesis pathway by *CerS6* knockdown after PDT is supported by the following data: all significant changes in dihydroceramides, products of CerS, were displayed as decreases in their levels, and the levels of the CerS substrate dihydrosphingosine were increased. The results are in accord with our previous observations showing that PDT regulates sphingolipid levels by this pathway and that *de novo* sphingolipids modulate the apoptotic response to PDT (10-12).

In summary, our present study indicates that CerS6 controls apoptotic susceptibility to PDT *via* the *de novo* sphingolipid biosynthesis pathway. These novel findings suggest that alterations in CerS expression might be utilized therapeutically to control resistance to PDT.

Acknowledgements

This work was supported by U.S. Public Health Service Grant R01 CA77475 from the National Cancer Institute, National Institutes of Health (DS) and the Veterans Administration Merit Awards from RR&D and BLRD programs (TIG). The MS-related work was performed by the Lipidomics Shared Resource (Medical University of South Carolina), supported by NCI grants: IPO1CA097132 and P30 CA 138313 and NIH/NCRR SC COBRE Grant P20 RR017677. Laboratory space for the Lipidomics Shared Resource was supported by the NIH, grant C06 RR018823 from the Extramural Research Facilities Program of the National Center for Research Resources. We thank Drs. Besim Ogretmen and Can Emre Senkal for helpful discussions of the manuscript.

References

1 Hannun YA and Obeid LM: Principles of bioactive lipid signalling: lessons from sphingolipids. Nat Rev Mol Cell Biol *9*: 139-150, 2008.

2 Strettoi E, Gargini C, Novelli E, Sala G, Piano I, Gasco P and Ghidoni R: Inhibition of ceramide biosynthesis preserves photoreceptor structure and function in a mouse model of retinitis pigmentosa. Proc Natl Acad Sci USA *107*: 18706-18711, 2010.

3 Tidhar R, Ben-Dor S, Wang E, Kelly S, Merrill AH Jr. and Futerman AH: Acyl chain specificity of ceramide synthases is determined within a region of 150 residues in the Tram-Lag-CLN8 (TLC) domain. J Biol Chem *287*: 3197-3206, 2012.
4 Hannun YA and Obeid LM: Many ceramides. J Biol Chem *286*: 27855-27862, 2011.
5 Mesicek J, Lee H, Feldman T, Jiang X, Skobeleva A, Berdyshev EV, Haimovitz-Friedman A, Fuks Z and Kolesnick R: Ceramide synthases 2, 5, and 6 confer distinct roles in radiation-induced apoptosis in HeLa cells. Cell Signal *22*: 1300-1307, 2010.
6 White-Gilbertson S, Mullen T, Senkal C, Lu P, Ogretmen B, Obeid L and Voelkel-Johnson C: Ceramide synthase 6 modulates TRAIL sensitivity and nuclear translocation of active caspase-3 in colon cancer cells. Oncogene *28*: 1132-1141, 2009.
7 Novgorodov SA, Chudakova DA, Wheeler BW, Bielawski J, Kindy MS, Obeid LM and Gudz TI: Developmentally regulated ceramide synthase 6 increases mitochondrial Ca^{2+} loading capacity and promotes apoptosis. J Biol Chem *286*: 4644-4658, 2010.
8 Senkal CE, Ponnusamy S, Rossi MJ, Bialewski J, Sinha D, Jiang JC, Jazwinski SM, Hannun YA and Ogretmen B: Role of human longevity assurance gene 1 and C18-ceramide in chemotherapy-induced cell death in human head and neck squamous cell carcinomas. Mol Cancer Ther *6*: 712-722, 2007.
9 Wang H, Maurer BJ, Liu YY, Wang E, Allegood JC, Kelly S, Symolon H, Liu Y, Merrill AH Jr., Gouaze-Andersson V, Yu JY, Giuliano AE and Cabot MC: N-(4-Hydroxyphenyl)retinamide increases dihydroceramide and synergizes with dimethylsphingo-sine to enhance cancer cell killing. Mol Cancer Ther *7*: 2967-2976, 2008.
10 Wispriyono B, Schmelz E, Pelayo H, Hanada K and Separovic D: A role for the *de novo* sphingolipids in apoptosis of photosensitized cells. Exp Cell Res *279*: 153-165, 2002.
11 Dolgachev V, Farooqui MS, Kulaeva OI, Tainsky MA, Nagy B, Hanada K and Separovic D: *De novo* ceramide accumulation due to inhibition of its conversion to complex sphingolipids in apoptotic photosensitized cells. J Biol Chem *279*: 23238-23249, 2004.
12 Dolgachev V, Nagy B, Taffe B, Hanada K and Separovic D: Reactive oxygen species generation is independent of *de novo* sphingolipids in apoptotic photosensitized cells. Exp Cell Res *288*: 425-436, 2003.
13 Oleinick N, Morris R and Nieminen AL: Photodynamic therapy-induced apoptosis. *In*: Apoptosis, Senescence, and Cancer. Gewritz DA, Grant S and Holt SE (eds.). New Jersey, Humana Press., pp. 557-578, 2007.
14 Castano AP, Mroz P and Hamblin MR: Photodynamic therapy and antitumour immunity. Nat Rev Cancer *6*: 535-545, 2006.
15 Henderson BW, Gollnick SO, Snyder JW, Busch TM, Kousis PC, Cheney RT and Morgan J: Choice of oxygen-conserving treatment regimen determines the inflammatory response and outcome of photodynamic therapy of tumors. Cancer Res *64*: 2120-2126, 2004.
16 Brenner JC, Graham MP, Kumar B, Saunders LM, Kupfer R, Lyons RH, Bradford CR and Carey TE: Genotyping of 73 UM-SCC head and neck squamous cell carcinoma cell lines. Head Neck *32*: 417-426, 2010.
17 Zhu Z, Xu X, Yu Y, Graham M, Prince ME, Carey TE and Sun D: Silencing heat shock protein 27 decreases metastatic behavior of human head and neck squamous cell cancer cells *in vitro*. Mol Pharm *7*: 1283-1290, 2010.
18 Separovic D, Semaan L, Tarca AL, Awad Maitah MY, Hanada K, Bielawski J, Villani M and Luberto C: Suppression of sphingomyelin synthase 1 by small interference RNA is associated with enhanced ceramide production and apoptosis after photodamage. Exp Cell Res *314*: 1860-1868, 2008.
19 Separovic D, Kelekar A, Nayak AK, Tarca AL, Hanada K, Pierce JS and Bielawski J: Increased ceramide accumulation correlates with down-regulation of the autophagy protein ATG-7 in MCF-7 cells sensitized to photodamage. Arch Biochem Biophys *494*: 101-105, 2010.
20 Cossarizza A, Baccarani-Contri M, Kalashnikova G and Franceschi C: A new method for the cytofluorimetric analysis of mitochondrial membrane potential using the J-aggregate forming lipophilic cation 5,5',6,6'-tetrachloro-1,1',3,3'-tetraethylbenzimidazolcarbocyanine iodide (JC-1). Biochem Biophys Res Commun *197*: 40-45, 1993.
21 Separovic D, Mann KJ and Oleinick NL: Association of ceramide accumulation with photodynamic treatment-induced cell death. Photochem Photobiol *68*: 101-109, 1998.
22 Separovic D, Saad ZH, Edwin EA, Bielawski J, Pierce JS, Buren EV and Bielawska A: C16-ceramide analog combined with Pc 4 photodynamic therapy evokes enhanced total ceramide accumulation, promotion of DEVDase activation in the absence of apoptosis, and augmented overall cell killing. J Lipids *2011*: 1-9, 2010.
23 Lam M, Oleinick NL and Nieminen AL: Photodynamic therapy-induced apoptosis in epidermoid carcinoma cells. Reactive oxygen species and mitochondrial inner membrane permeabilization. J Biol Chem *276*: 47379-47386, 2001.
24 Senkal CE, Ponnusamy S, Bielawski J, Hannun YA and Ogretmen B: Antiapoptotic roles of ceramide-synthase-6-generated C16-ceramide *via* selective regulation of the ATF6/CHOP arm of ER-stress-response pathways. FASEB J *24*: 296-308, 2010.
25 Senkal CE, Ponnusamy S, Manevich Y, Meyers-Needham M, Saddoughi SA, Mukhopadyay A, Dent P, Bielawski J and Ogretmen B: Alteration of ceramide synthase 6/C16-ceramide induces activating transcription factor 6-mediated endoplasmic reticulum (ER) stress and apoptosis *via* perturbation of cellular Ca^{2+} and ER/Golgi membrane network. J Biol Chem *286*: 42446-42458, 2011.
26 Agarwal ML, Clay ME, Harvey EJ, Evans HH, Antunez AR and Oleinick NL: Photodynamic therapy induces rapid cell death by apoptosis in L5178Y mouse lymphoma cells. Cancer Res *51*: 5993-5996, 1991.
27 Mizutani Y, Kihara A and Igarashi Y: Mammalian Lass6 and its related family members regulate synthesis of specific ceramides. Biochem J *390*: 263-271, 2005.
28 Koybasi S, Senkal CE, Sundararaj K, Spassieva S, Bielawski J, Osta W, Day TA, Jiang JC, Jazwinski SM, Hannun YA, Obeid LM and Ogretmen B: Defects in cell growth regulation by C18:0-ceramide and longevity assurance gene 1 in human head and neck squamous cell carcinomas. J Biol Chem *279*: 44311-44319, 2004.
29 Mullen TD, Jenkins RW, Clarke CJ, Bielawski J, Hannun YA and Obeid LM: Ceramide synthase-dependent ceramide generation and programmed cell death: involvement of salvage pathway in regulating postmitochondrial events. J Biol Chem *286*: 15929-15942, 2011.

Received January 4, 2012
Revised February 7, 2012
Accepted February 8, 2012